Journal of Mechanics in Medicine and Biology
Vol. 2, Nos. 3 & 4 (2002) 1–7

APONEUROSIS LENGTH AND FASCICLE INSERTION ANGLES OF THE BICEPS BRACHII

DEANNA S. ASAKAWA[*,†], GEORGE P. PAPPAS[*,†],
SCOTT L. DELP[*,‡] and JOHN E. DRACE[†]

[*]*Biomechanical Engineering Division, Mechanical Engineering Department,*
Stanford University, Stanford, California, 94305-3030

[†]*Diagnostic Radiology Center, VA Palo Alto Health Care System, Palo Alto, California*
[‡]*delp@stanford.edu*

Received 000
Accepted 000

Magnetic resonance images and ultrasound images were used to examine the architecture of the distal biceps brachii muscle in 12 unimpaired subjects. The distal biceps brachii tendon continued as an internal aponeurosis that spanned $34 \pm 4\%$ of the length of the biceps brachii long head muscle on average. The distal muscle fascicles inserted at angles to this aponeurosis; fascicles anterior to the aponeurosis inserted at a significantly greater ($p \leq 0.05$) angle (17°) than the fascicles posterior to the aponeurosis (14°) in the distal 2 cm of muscle when the elbow was extended. Mean fascicle insertion angles were on average 3–4° greater with the elbow flexed 90° against a 5% maximum voluntary contraction load as compared to their values with the elbow extended. These data provide the basis for designing experiments to measure muscle and tendon motion *in vivo*.

Keywords: Muscle; biceps brachii; magnetic resonance imaging; ultrasound.

1. Introduction

Mathematical models of muscle generally assume the muscle fascicles shorten uniformly along their length. Unfortunately, there have been few *in vivo* studies that test the accuracy of this assumption, primarily because of limitations in experimental methods. Cine phase contrast magnetic imaging (cine-PC MRI) is a technique that allows accurate measurement of muscle and tendon motion *in vivo*.[1,2] This dynamic imaging technique allows measurement of the three-dimensional velocity of the muscle tissue and calculation of the percent shortening within different regions of the muscle. Using these measurements, the common assumption that muscle shortens uniformly along its length can be tested.[3] However, measurement of the amount of shortening along a fascicle with cine-PC MRI requires knowledge of the orientation of the muscle fascicles, the change in fascicle orientation with muscle shortening, and the extent of the aponeurosis.

Previous studies have used ultrasound to non-invasively characterize features of muscle such as pennation angle, fascicle length, muscle thickness and moment arm.[4–10] Ultrasound images have revealed changes in pennation with fascicle shortening and force development *in vivo*.[11–13] To date, ultrasound investigations of pennation angle in the upper limb muscles have been limited to the brachialis and the triceps brachii.[8,11] For the biceps brachii, the length of the aponeurosis and the orientation of the fascicles with respect to the aponeurosis are unknown.

The purpose of this study, therefore, was to characterize (i) the extent of the distal aponeurosis within the biceps brachii muscle, (ii) the orientation of the distal fascicles with respect to the aponeurosis, and (iii) the change in orientation of the fascicles with flexion of the elbow. This study provides *in vivo* geometry measurements for the biceps brachii muscle.

2. Methods

We used static magnetic resonance images and ultrasound images to study the biceps brachii architecture. Static MR images of the biceps brachii were acquired of the right arms of 12 subjects (10 male, 2 female) with a 1.5T scanner (GE Medical Systems, Milwaukee, WI). Average anthropometric characteristics of the subjects are presented in Table 1. The Institutional Review Board at Stanford University approved the imaging protocols, and informed consent was obtained from each subject in accordance with institutional policy.

T2-weighted MR images were acquired in an axial plane with a fast spin echo sequence (2000 msec repetition time, 2 excitations, 12 cm $\times$ 12 cm field of view, 256 $\times$ 160 pixel matrix) and 7-mm slice thickness at 10-mm intervals along the upper arm with the elbow near full extension ($\leq 10°$ flexion). These images were analyzed using GE image analysis software to estimate the extent of the distal aponeurosis within the muscle and the length of the biceps brachii long head muscle belly. Aponeurosis length was measured as the distance from the distal myotendinous

Table 1. Characteristics of the twelve subjects.

Measurement	Mean (SD)
Age (years)	30 (7)
Height (cm)	181.9 (11.6)
Weight (kg)	72.9 (6.9)
MVC (kg)[a]	21.7 (4.4)
Arm length (cm)[b]	32.9 (1.6)
Arm circumference (cm)[c]	32.6 (2.6)

[a]Maximum voluntary contraction load with 90° elbow flexion. See text for details.
[b]Upper arm length measured from the lateral edge of the acromion to lateral humeral epicondyle.
[c]Arm circumference measured as the maximum with the elbow flexed 90° in weak isometric contraction.

junction to the most proximal image in which aponeurosis was visible (Fig. 1). Similarly, the length of the biceps brachii long head muscle was estimated as the distance between the distal myotendinous junction and most proximal image in which muscle tissue was evident.

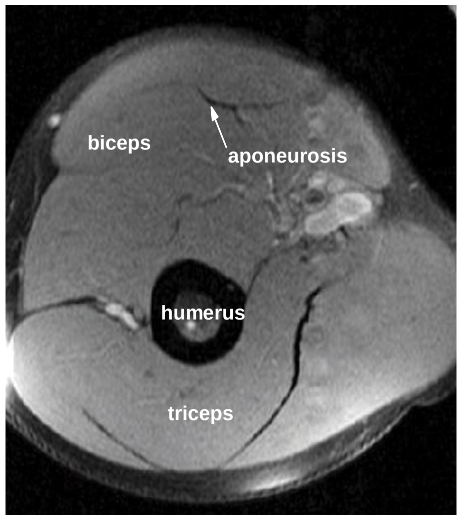

Fig. 1. Axial MR image of the upper arm of one subject showing the biceps brachii (top) and the sheet-like distal aponeurosis through the central section of the muscle. We measured biceps brachii muscle length and aponeurosis length as the distance between the most inferior and the most superior MR images in which muscle tissue or aponeurosis tissue was visible respectively.

We acquired ultrasound images of the biceps brachii from the same subjects with the elbow extended and with the elbow flexed 90° while the subject resisted a load equal to 5% of their maximum voluntary contraction (MVC) strength. The load was applied using a calibrated elastic cord. MVC strength was measured for each subject using a spring gauge with the subject standing and the elbow flexed 90°. An Acuson Sequoia 512 Ultrasound System (Mountain View, CA) with a 52-mm wide, 15-MHz transducer was used to obtain the images. The transducer was oriented to produce mid-sagittal plane images of the biceps brachii with the distal aponeurosis evident (Fig. 2). The angle of the probe with respect to the muscle was varied slightly to produce images that clearly showed individual muscle fascicle boundaries and the fascicle's insertion into the aponeurosis. Between 10 to 20 images were taken for each of the two elbow positions for each subject.

NIH Image software (U.S. National Institutes of Health) was used to measure the angles at which fascicles inserted into the aponeurosis. We recorded fascicles insertion angles in the distal biceps brachii muscle in two separate regions: 0–2 cm and 2–4 cm proximal to the point where the most distal fiber inserted into

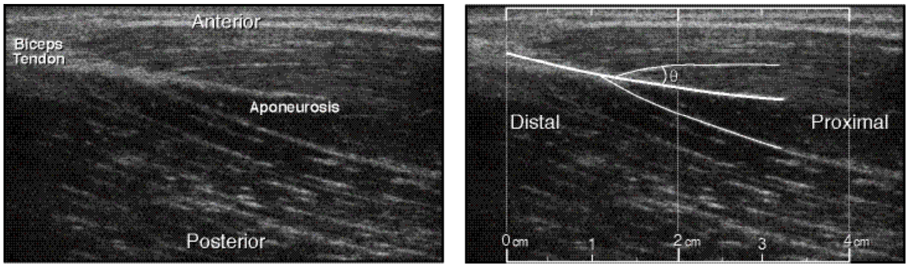

Fig. 2. Mid-sagittal plane ultrasound image of the distal biceps brachii; the distal biceps tendon (upper left) continues as an internal aponeurosis. Fascicles are visible inserting into the aponeurosis from the anterior and posterior aspects of the muscle (left frame). Fascicle insertion angles anterior and posterior to the aponeurosis were measured in two regions, 0–2 cm from the distal myotendinous junction or 2–4 cm from the distal myotendinous junction using NIH Image software (right frame).

the tendon. Angles of fascicles both anterior and posterior to the aponeurosis were measured. The insertion angles of 2–5 fascicles in each of the four regions (anterior 0–2 cm, anterior 2–4 cm, posterior 0–2 cm, posterior 2–4 cm) were measured for each subject.

We compared the insertion angles of fascicles anterior to the aponeurosis to insertion angles of fascicles posterior to the aponeurosis using a paired t-test. A paired t-test was also performed to examine differences in fascicle insertion angles when the elbow was extended as compared to fascicle insertion angles when the elbow was flexed resisting a low-level load.

3. Results

The distal internal aponeurosis spanned $34 \pm 4\%$ of the length of the biceps brachii muscle on average. The average aponeurosis length was 7 ± 1 cm in the 12 subjects. The length of the biceps brachii long head muscle averaged 20 ± 2 cm with the elbow within 10° of full extension.

There was asymmetry in the anterior and posterior fascicle insertion angles. The average insertion angle for fascicles anterior to the aponeurosis was 17° for the distal 2 cm of the muscle with the elbow extended (Table 2). The posterior fascicles in this same region inserted at 14° with the elbow extended. Fascicles anterior to the aponeurosis inserted at a significantly greater ($p \leq 0.05$) angle than the fascicles posterior to the aponeurosis in both regions (0–2 cm and 2–4 cm) when the elbow was extended. With the elbow flexed, resisting 5% MVC, only fascicles within the distal 0–2 cm of the muscle showed significant asymmetry in anterior and posterior insertion angles.

Fascicle insertion angles with the elbow flexed while resisting 5% MVC were significantly larger ($p \leq 0.05$) than angles measured with the elbow extended for all regions of the muscle studied. For example, fascicle insertion angles anterior to

Table 2. Fascicle insertion angles in degrees for the distal biceps brachii.

	Elbow Extended		Elbow Flexed 90° (*resisting 5% MVC*)	
	mean (SD)	range	mean (SD)	range
Anterior fascicles				
Distal 0–2 cm	17 (4)	11–24	21 (4)	16–30
Distal 2–4 cm	14 (3)	10–21	17 (4)	12–24
Posterior fascicles				
Distal 0–2 cm	14 (3)	8–18	18 (4)	12–24
Distal 2–4 cm	12 (2)	8–14	15 (3)	12–21

the aponeurosis increased with elbow flexion from 17° to 21° in the distal 0–2 cm of the muscle and from 14° to 17° in the distal 2–4 cm of the muscle. This increase in fascicle insertion angle with elbow flexion was small but consistent across subjects.

4. Discussion

Characterizing the *in vivo* architecture of a muscle is an important first step in understanding the functional implications of a specific muscle's architecture.[7,14–16] For example, a muscle's force-length and force-velocity relationships depend on the spatial arrangement of fascicles within the muscle. In a pennate muscle, the change in muscle length with contraction, and the force transmitted to the tendon, are influenced by the amount of pennation and the change in pennation angle with contraction.[17,18] The data presented in this study are needed to accurately model these complexities of the distal biceps brachii architecture.

We measured the length of the biceps brachii long head and the length of the aponeurosis from axial MR images as the distance between the most superior and most inferior images in which muscle or aponeurosis tissue was visible. However, the 10-mm distance between axial images limited the resolution of these length measurements. Murray *et al.*[19] reported a 21.6 ± 4.5 cm mean optimal muscle length for the biceps brachii long head measured from 10 upper extremity cadaver specimens, similar to the 20 ± 2 cm average biceps brachii long head length measured with the elbow near full extension in this study. We used this estimate of the biceps brachii long head length to gauge what percentage of the muscle length contained aponeurosis tissue. We expect that the presence of the aponeurosis, which is less compliant than the muscle tissue,[20–22] will influence the motion of the muscle tissue during contraction.

We found significant changes in fascicle insertion angle for the biceps brachii with a 90° change in elbow angle accompanied by low-load contraction. Herbert and Gandevia[11] showed that there was no effect of elbow angle on pennation when the brachialis muscle was relaxed. However, similar to our findings in the biceps brachii, they reported a marked increase in pennation angle in the brachialis muscle with a 90° change in elbow angle with loads as low as 10% MVC. While we observed the increase in fascicles insertion angles in the biceps brachii, we do not know if this is due to shortening or force development in the muscle.

Use of magnetic resonance images and ultrasound images enabled us to describe the extent of the aponeurosis, the orientation of fascicles with respect to the aponeurosis, and the change in fascicle orientation *in vivo*. Characterization of the extent of the distal aponeurosis of the biceps brachii and the orientation of the fascicles with respect to this aponeurosis is required to interpret the contraction mechanics using cine-PC MRI. For example, knowledge of the arrangement and orientation of the fascicles would allow one to estimate change in length along a fascicle given *in vivo* tissue motion data. This description of the trajectory of fascicles within the distal biceps brachii provides new information that is needed to design experiments and analyze the *in vivo* muscle and tendon motion for this muscle.

Acknowledgments

Funding was provided by the National Institutes of Health (grants ROI-HD31493 and ROI-HD38962), the Department of Veterans Affairs, a Stanford-NIH Biotechnology Training Grant Program Fellowship, and a Whitaker Foundation Graduate Fellowship.

References

1. Sheehan, F. T., Zajac, F. E. and Drace, J. E., Using cine phase contrast magnetic resonance imaging to non-invasively study *in vivo* knee dynamics, *J. Biomech.* **31** (1998) 21–26.
2. Drace, J. E. and Pelc, N. J., Skeletal muscle contraction: analysis with use of velocity distributions from phase-contrast MR imaging, *Radiology* **193** (1994) 423–429.
3. Pappas, G., Asakawa, D. S., Delp, S. L., Zajac, F. E. and Drace, J. E., Nonuniform shortening in the biceps brachii during elbow flexion, *J. Appl. Physiol.* **92** (2002) 2381–2389.
4. Fukunaga, T., Ichinose, Y., Ito, M., Kawakami, Y. and Fukahiro, S., Determination of fascicle length and pennation in contracting human muscle *in vivo*, *J. Appl. Physiol.* **82**(1) (1997) 354–358.
5. Henriksson-Larsen, K., Wretling, M. L., Lorentzon, R. and Oberg, L., Do muscle fibre size and fibre angulation correlate in pennated human muscles? *Eur. J. Appl. Physiol.* **64** (1992) 68–72.
6. Ito, M., Akima, H. and Fukunaga, T., *In vivo* moment arm determination using B-mode ultrasonography, *J. Biomech.* **33** (2000) 215–218.
7. Narici, M., Human skeletal muscle architecture studied *in vivo* by non-invasive imaging techniques: functional significance and applications, *J. Electromyography Kinesiology* **9** (1999) 97–103.
8. Kawakami, Y., Abe, T. and Fukunaga, T., Muscle-fiber pennation angles are greater in hypertrophied than in normal muscles, *J. Appl. Physiol.* **74** (1993) 2740–2744.
9. Rutherford, O. M. and Jones, D. A., Measurement of fibre pennation using ultrasound in the human quadriceps *in vivo*, *Eur. J. Appl. Physiol.* **65** (1992) 433–437.

10. Maganaris, C. N., *In vivo* measurement-based estimations of the moment arm in the human tibialis anterior muscle-tendon unit, *J. Biomech.* **33** (2000) 375–379.
11. Herbert, R. D. and Gandevia, S. C., Changes in pennation with joint angle and muscle torque: *in vivo* measurements in human brachialis muscle, *J. Physiol.* **484**(2) (1995) 523–532.
12. Fukunaga, T., Kawakami, S. K., Funato, K. and Fukashiro, S., Muscle architecture and function in humans, *J. Biomech.* **30**(5) (1997) 457–463.
13. Kawakami, Y., Yoshiho, I., Kubo, K., Ito, M., Imai, M. and Fukunaga, T., Architecture of contracting human muscles and its functional significance, *J. Appl. Biomech.* (2000) **16** 88–98.
14. Lieber, R. L., Loren, G. J. and Friden, J., *In vivo* measurement of human wrist extensor muscle sarcomere length changes, *J. Neurophysiology* **71**(3) (1994) 874–881.
15. Scott, S. H., Engstrom, C. M. and Loeb, G. E., Morphology of human thigh muscles. Determination of fascicle architecture by magnetic resonance imaging, *J. Anatomy* **182** (1993) 249–257.
16. van Doorn, A., Bovendeerd, P. H. M., Nicolay, K., Drost, M. R. and Janssen, J. D., Determination of muscle fibre orientation using diffusion-weighted MRI, *Eur. J. Morph.* **34**(1) (1996) 5–10.
17. Zajac, F. E., Muscle and tendon: properties, models, scaling, and application to biomechanics and motor control, *CRC Critical Reviews Biomedical Engineering* **17**(4) (1989) 359–411.
18. Delp, S. L. and Zajac, F. E., Force- and moment-generating capacity of lower-extremity muscles before and after tendon lengthening, *Clin. Orthop. Rel. Res.* **284** (1992) 247–259.
19. Murray, W. M., Buchanan, T. and Delp, S., The isometric functional capacity of muscles that cross the elbow, *J. Biomech.* **33**(8) (2000) 943–952.
20. Zuurbier, C. J. and Huijing, P. A., Influence of muscle geometry on shortening speed of fibre, aponeurosis and muscle, *J. Biomech.* **25** (1992) 1017–1026.
21. Lieber, R. L., Leonard, M. E., Brown, C. G. and Tresik, C. L., Frog semitendinosis tendon load-strain and stress-strain properties during passive loading, *Am. J. Physiol.* **261** (1991) C86–92.
22. Ettema, G. J. and Huijing, P. A., Properties of the tendinous structures and series elastic component of EDL muscle-tendon complex of the rat, *J. Biomech.* **22** (1989) 1209–1215.